RSC Advances

PAPER

View Article Online
View Journal | View Issue

Cite this: *RSC Adv.*, 2020, **10**, 43950

Influence of the physicochemical features of TiO_2 nanoparticles on the formation of a protein corona and impact on cytotoxicity†

Ozge Kose, Marion Stalet, Lara Leclerc and Valérie Forest *

Received 2nd October 2020
Accepted 24th November 2020

DOI: 10.1039/d0ra08429h

rsc.li/rsc-advances

Due to their unique properties TiO_2 nanoparticles are widely used. The adverse effects they may elicit are usually studied in relation to their physicochemical features. However, a factor is often neglected: the influence of the protein corona formed around nanoparticles upon contact with biological media. Indeed, although it is acknowledged that it can strongly influence nanoparticle toxicity, it is not systematically considered. The aim of this study was to characterize the formation of the protein corona of TiO_2 nanoparticles as a function of the main nanoparticle properties and investigate potential relationship with the cytotoxicity nanoparticles induce *in vitro* in human lung cells. To that purpose, five TiO_2 nanoparticles differing in size, shape, agglomeration state and surface charge were incubated in cell culture media (DMEM or RPMI supplemented with 10% fetal bovine serum) and the amount and profile of adsorbed proteins on each type of nanoparticle were compared to their toxicological profile. While nanoparticle size and surface charge were found to be determinant factors for protein corona formation, no clear impact of the shape and agglomeration state was observed. Furthermore, no clear relationship was evidenced between the protein corona of the nanoparticles and the adverse effect they elicited.

1. Introduction

Titanium dioxide (TiO_2) nanoparticles are among the most produced and industrially used nanoparticles.[1] Because their small size confers unique properties, they are used in a wide range of application fields. They are for instance characterized by their brightness/whiteness, high refractive index, opacifying strength, resistance to discoloration, self-cleaning and antifogging property, ultraviolet block capacity, catalytic properties and antimicrobial activity.[2–5] Many applications can take advantage of these properties, both in the industrial sector and in daily-life consumer products. Thus, TiO_2 nanoparticles can be used as pigment, catalyst, in paints, papers, inks, plastics, rubber industry, solar cells, construction material, self-cleaning roof tiles and windows, anti-fogging car mirrors, textile, as food additive (E171), in personal care products (toothpaste, cosmetics, sunscreens), in environmental or biomedical applications (photocatalytic degradation of pollutants, air and water purification, biosensing, drug delivery) and even in pharmaceuticals.[1,2,4–6]

Initially considered as biologically inert, titanium dioxide was classified as "possibly carcinogen to humans" (Group 2B) by the International Agency for Research on Cancer (IARC).[2] However, it remains a controversial issue as there is not only one type of TiO_2 nanoparticles but several depending on their physicochemical features and conclusions can hardly be generalized. Indeed, the biological impact of nanoparticles is directly influenced by their physicochemical characteristics.[7,8] We previously assessed the cytotoxicity induced by TiO_2 nanoparticles on human lung cell lines in relation to their physicochemical features.[9] We observed a higher toxicity with bigger sized, less agglomerated, rod-shaped, and positively charged TiO_2 nanoparticles, confirming that nanoparticle toxicity is directly correlated with their physicochemical features.

However, to fully understand this relationship, another factor has to be considered: the formation of a protein corona. Indeed, upon contact with biological media, the biomolecules they contain, and especially proteins, rapidly adsorb on the nanoparticle surface forming a crown, the so-called corona. This formation is directly influenced both by the biological environment (medium composition and factors such as temperature, pH, duration of incubation, *etc.*) and by the nanoparticle physicochemical features (especially, size, shape, surface charge and hydrophobicity).[10–21] The protein corona represents the new interface between nanoparticles and biological systems and will thus have a strong impact on their interactions and the subsequent cell response. The pristine nanoparticle being "screened" by the proteins adsorbed on its surface, interactions with biological systems will be made through this protein layer and not with bare materials.[22] It will

Mines Saint-Etienne, Univ Lyon, Univ Jean Monnet, INSERM, U1059 Sainbiose, Centre CIS, F-42023 Saint-Etienne Cedex 2, France. E-mail: vforest@emse.fr

† Electronic supplementary information (ESI) available. See DOI: 10.1039/d0ra08429h

consequently determine the physiological behavior of nanoparticles, triggering vast biological outcomes.[13,23,24]

It is commonly acknowledged that the protein corona generally mitigates the cytotoxicity induced by nanoparticles[23–28] as a consequence of a lower cell uptake.[29–37] However, some studies have shown on the contrary that the presence of a protein corona can enhance the nanoparticle cytotoxicity.[38]

In any way, a better characterization of the nanoparticle corona is of paramount importance to better understand the biological effects of nanoparticles. The aim of this study was to characterize the formation of the protein corona of TiO_2 nanoparticles as a function of the main nanoparticle properties and investigate potential relationship with the cytotoxicity nanoparticles induce *in vitro* in human lung cell lines. To that purpose, 5 TiO_2 nanoparticles differing in size, shape, agglomeration state and surface charge were incubated in cell culture media and the amount and profile of adsorbed proteins on each type of nanoparticle were compared to their toxicological profile.

2. Materials and methods

Our approach is summarized in Fig. 1.

The protocol used for the semi-quantitative analysis of the protein corona composition of TiO_2 nanoparticles was inspired from Docter *et al.*[39] but was adapted to our nanoparticles and conditions.

2.1. Nanoparticles

Five types of TiO_2 nanoparticles were used in this study. In addition to commercial P25 nanoparticles (Evonik P25 CAS: 1317-70-0, Sigma-Aldrich, France) used as a reference, four types of TiO_2 nanoparticles were synthesized with different and well-controlled physicochemical properties. They were referred to as S1 to S4 and differed in size, shape, agglomeration state and surface functionalization/charge. They were synthesized using Chen *et al.* method.[40] Basically, titanium(IV) butoxide (CAS: 5593-70-4 reagent grade 97%, Sigma-Aldrich, Saint-Quentin-Fallavier, France) was mixed with triethanolamine (CAS: 102-71-6, Analytical reagent 97%, VWR International, Fontenay-sous-Bois, France) in 1 : 2 molar ratio. The mixture was put in Teflon lined sealed autoclave and then heated at 150 °C during 24 h. The pH values of the synthesis medium were adjusted using HCl or NH_4OH to tune particle size and morphology. Finally, the solutions were washed by three centrifugations using de-ionized water and the resulting products were dried in an oven at 40 °C. Surface functionalization of S2 nanoparticles was generated by aminopropyltriethoxysilane (APTES) using Zhao *et al.* method.[41] Briefly, 0.25 g of S2 nanopowder was dispersed in 25 mL de-ionized water by ultrasonication for 10 min. Then, the silane coupling agents APTES were added in the dispersion (molar ratio of 1 : 1). The mixture was sonicated until a clear solution was obtained and then refluxed at 80 °C for 4 h. After that, dispersed particles were separated from solvent by centrifugation (10 min at 1200*g*) followed by washing with water at least 2 times. The final functionalized samples were then prepared in de-ionized water and labeled as S4.

Stock suspensions of all nanoparticles (1600 μg mL^{-1}) were prepared in de-ionized water (MilliQ systems, Millipore, Bedford, MA, USA) and sonicated with Branson Sonifier S-450 for 10 min at 89% amplitude. Nanoparticles were then extensively characterized.[9] The morphology and size distribution of the

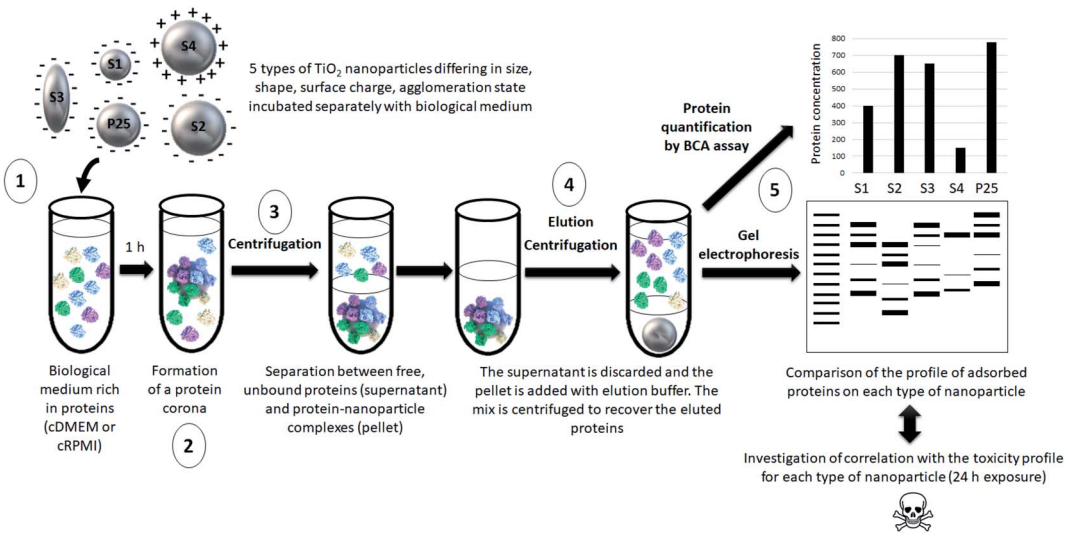

Fig. 1 Schematic representation of the main steps of our approach. (1) 5 types of nanoparticles characterized by different physicochemical features were incubated in a biological fluid (cell culture medium) for 1 h. (2) Proteins from this biological environment adsorbed at the nanoparticle surface forming the so-called protein corona. (3) The nanoparticle–protein complexes were separated from unbound proteins by centrifugation. (4) Proteins were then eluted from nanoparticles and (5) quantified by a protein assay and analyzed by gel electrophoresis. The profile of adsorbed proteins was discussed with regard to the physicochemical features of the nanoparticles and potential correlations with their previously assessed toxicity profile were investigated.

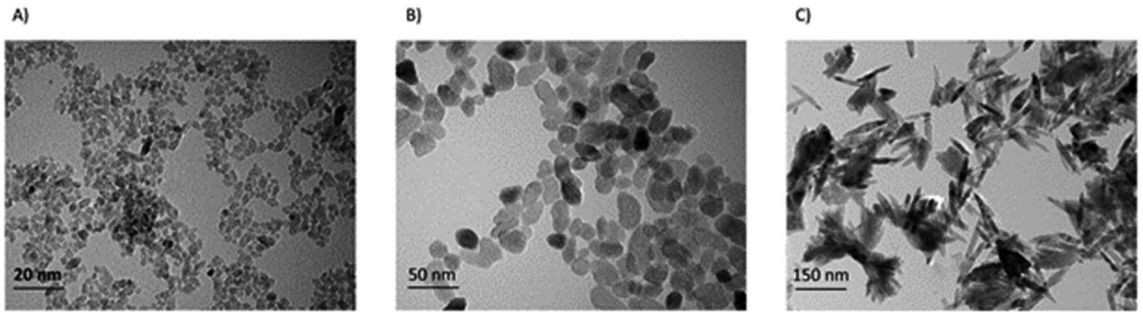

Fig. 2 Transmission electron microscope images of S1 (A), S2 (B), and S3 (C) TiO_2 nanoparticles.

Table 1 Particle primary size (TEM), specific surface area (SSA, BET), shape (TEM, SEM), and crystal structure (XRPD)

	Primary size (nm)	SSA (m^2 g^{-1})	Particle shape	Crystal structure	Surface coating
S1	15	146	Spherical	Anatase	No
S2	30	61	Spherical	Anatase	No
S3	20–250[a]	41	Rod	Anatase	No
S4	30	61	Spherical	Anatase	APTES[b]
P25	21	55	Spherical	Anatase: Rutile (90 : 10)	No

[a] Minimum and maximum Feret diameters. [b] APTES coating was carried out on S2 nanoparticles to obtain S4 nanoparticles.

nanoparticles were analyzed by transmission electron microscopy (TEM) using a FEI TECNAI 20FST operating at 200 kV and scanning electron microscopy (SEM) at 2–3 kV on a Zeiss Sigma 300 microscope using a secondary electron detector. Fig. 2 illustrates the morphology of the nanoparticles. After each TEM image of each sample were chosen, the size distribution and the mean diameter were measured by ImageJ software.

The hydrodynamic size and the agglomeration status of the TiO_2 nanoparticles (120 μg mL^{-1}) in de-ionized water and in culture media were determined by using dynamic light scattering (DLS, Zetasizer Nano ZS Malvern Instruments, Worcestershire, UK) measurements. Surface charge of the nanoparticles was monitored using electrophoretic light scattering (ELS, Zetasizer Nano ZS Malvern Instruments, Worcestershire, UK). Specific surface areas (SSA) were measured by linearizing the physisorption isotherm of N_2 at 77 K with the classical method of Brunauer, Emmett and Teller (BET) (Volumetric Adsorption ASAP 2020, Micrometrics, USA).[42]

Tables 1 and 2 summarize the main physicochemical features of the nanoparticles. DLS graphs can be found in ESI.†

2.2. Biological media

Two types of cell culture media were used: Dulbecco's Modified Eagle Medium (DMEM) high glucose (4.5 g L^{-1}) with stable glutamine and sodium pyruvate (cat. no. L0103-500, VWR International, France) and Roswell Park Memorial Institute (RPMI 1640) with L-glutamine (cat. no. L0500-500, Gibco, Life Technologies, France). Both media were supplemented with 10% (v/v) fetal bovine serum (FBS, cat. no. S1810-500, Biowest, France, for the reproducibility of the results, we ensured that all FBS aliquots came from the same batch) and 1% penicillin-streptomycin (VWR International, France). Once supplemented, media were called complete and referred to as cDMEM and cRPMI respectively.

2.3. Nanoparticles/biological media contact

To ensure comparability between the results the ratio of total particle–surface area to the biological medium volume has to be kept constant for all nanoparticles. After preliminary experiments, we established that the optimal ratio was 0.1 m^2 mL^{-1} in a final volume of 4 mL. Based on the nanoparticle surface specific area (SSA), we calculated for each nanoparticle type the volume of stock solution to dilute in culture medium as reported in Table 3. TiO_2 nanoparticles were incubated either in cRPMI or cDMEM for 1 h at 37 °C.

2.4. Removal of unbound proteins

Samples were centrifuged 1 h at 14 100*g* (Mini-centrifuge MiniSpin Plus, VWR International, Fontenay-sous-Bois, France) at room temperature to separate the nanoparticle–protein complexes from the cell culture medium. The supernatant was discarded and the pellets were washed with 1 mL PBS to remove the proteins that did not bound tightly to the nanoparticles, the tubes were sonicated (Branson Sonifier S-450, amplitude 89%, pulse 2 s and intervals 2 s). Two additional washes consisting of a 20 min centrifugation at 14 100*g*, room temperature were carried out. The supernatant was finally discarded and the pellet containing the nanoparticle–protein complexes was used for the next step.

2.5. Recovery of the proteins adsorbed at the surface of the nanoparticles

Proteins were eluted from the nanoparticle–protein complexes by adding 300 μL of Laemmli buffer containing 62.5 mM Tris,

Table 2 Average hydrodynamic size, polydispersity index (PDI) and zeta potential in deionized water (DI H_2O) and in culture media (cDMEM and cRPMI) after dispersion of TiO_2 nanoparticles (120 μg mL^{-1}). All data are presented as means of three independent characterizations ± standard deviation

	DI H_2O		cDMEM		cRPMI	
	Average hydrodynamic size[a] (nm) (PDI)	Zeta potential (mV) pH 7.5	Average hydrodynamic size[a] (nm) (PDI)	Zeta potential (mV) pH 7.5	Average hydrodynamic size[a] (nm) (PDI)	Zeta potential (mV) pH 7.5
S1	211.4 ± 2.3 (0.15)	−15.8 ± 4.0	226 ± 9.1 (0.28)	−33.8 ± 1.8	241.4 ± 3.0 (0.22)	−12.6 ± 1.6
S2	969.3 ± 39.5 (0.27)	−13.8 ± 4.4	1094 ± 46.4 (0.36)	−31.0 ± 0.3	1138 ± 35.9 (0.328)	−11.8 ± 0.6
S3	1409 ± 89.6 (0.11)	−13.2 ± 4.2	1275 ± 66.6 (0.18)	−32.0 ± 3.0	1267 ± 111.5 (0.42)	−10.9 ± 0.1
S4	1204 ± 59.9 (0.16)	+12.3 ± 0.5	1398 ± 54.9 (0.48)	−36.6 ± 4.5	1515 ± 16.01 (0.312)	−11.4 ± 0.6
P25	256.4 ± 136.6 (0.27)	−15.2 ± 5.3	325 ± 4.1 (0.26)	−28.1 ± 0.6	434.6 ± 21.1 (0.33)	−11.9 ± 0.5

[a] Dynamic light scattering (DLS) measurements are the mean of at least 3 runs each containing 20 sub-measurements.

Table 3 Preparation of nanoparticle samples for cell culture media contact. The final nanoparticle–surface area ratio was 0.1 m^2 mL^{-1}. NP: Nanoparticle

NP type	SSA (m^2 g^{-1})	NP stock solution concentration (μg mL^{-1})	NP stock volume (μL)	Cell culture medium volume (μL)	Total volume (μL)
S1	146.5	16 000	171	3829	4000
S2	61.02	16 000	410	3590	4000
S3	40.78	16 000	613	3387	4000
S4	61.02	16 000	410	3590	4000
P25	55.00	16 000	455	3545	4000

5% (vol/vol) glycerol, 2% (wt/vol) SDS. After a 5 min incubation at 95 °C, the samples were centrifuged for 15 min at 14 100*g* at room temperature. The supernatant containing the eluted corona proteins was transferred into an Eppendorf Protein Lobind tube and used for protein quantification and gel electrophoresis as described below.

2.6. Determination of protein concentration

The protein concentration was assessed in the supernatant using a BCA protein assay kit (Pierce, Thermo Fisher Scientific, France) according to the manufacturer's instructions. Briefly, in a microplate 25 μL of solution were transferred per well and added with 200 μL of reagents from the kit. The plate was shaken for 30 s, covered and incubated at 37 °C for 30 min. After cooling to room temperature, the absorbance at 562 nm was read with a microplate spectrophotometer (Multiskan, Thermo Fisher Scientific, France). Calculation of protein concentrations was based on the use of a standard curve established with BSA (protein standard included in the kit). Results are means of three independent experiments each performed in duplicate.

2.7. Determination of the profile of proteins adsorbed at the surface of the nanoparticles by gel electrophoresis

30 μL of sample was added with 10 μL of 4× Bolt LDS sample buffer Novex (Invitrogen, Thermo Fisher Scientific, France). The mix was heated at 70 °C for 10 min. Samples were loaded in precast polyacrylamide gels (Invitrogen Bolt Bis-Tris Plus 4–12%, 10 wells, Thermo Fisher Scientific, France). A well was filled with 10 μL protein markers (SeeBlue Plus2 pre-stained protein standard Novex, Thermo Fisher Scientific, France). 1× running buffer was prepared by mixing 50 mL of 20× Bolt MES SDS Novex (Invitrogen, Thermo Fisher Scientific, France) with 950 mL of deionized water. The gel was run at room temperature, at 200 V constant for 22 min. It was then directly transferred into the Instant Blue staining solution (cat. no. ISB1L, Expedeon) for 1 h at room temperature with gentle shaking. A picture of the gel was taken. Three independent experiments were performed.

2.8. Nanoparticle cytotoxicity assessment

The cytotoxicity of the TiO_2 nanoparticles was previously assessed[9] on a human lung coculture system consisting of A549 epithelial cells and THP-1 differentiated macrophages cultivated in cDMEM. After a 24 h cell exposure to 15, 30, 60 or 120 μg mL^{-1} of nanoparticles, cytotoxicity was assessed in terms of cell viability (Trypan blue exclusion assay), pro-inflammatory response (production of the IL-8 and TNF-α cytokines assessed by commercial ELISA kits) and oxidative stress (production of reactive oxygen species, ROS detected by the cell-permeable fluorogenic probe 2′,7′-dichlorodihydrofluorescin diacetate, DCFH-DA).

2.9. Statistical analysis

For protein quantification, unless otherwise stated, results are expressed as mean of 3 independent experiments, each performed in duplicate ± standard deviation (SD). Statistical

analyses were performed using GraphPad Prism® (version 8.0, GraphPad Software, San Diego, CA, USA). Statistical analyses were conducted using a one-way Anova analysis followed by a Tukey's multiple comparison test. Differences were considered statistically significant when $P < 0.05$. The amount of proteins found in the corona of S1 and S3 was compared to that of the P25 reference. The amount of proteins found in the corona of S2 was compared to that of S4, its APTES-functionalized counterpart. Finally, the protein amount was compared between protein coronas formed in cDMEM and those formed in cRPMI for each sample.

3. Results

3.1. Protein concentration

Fig. 3 reports the mean concentrations of proteins eluted from the corona of the different nanoparticles incubated either in cDMEM or cRPMI.

For both media, proteins were less abundantly found in the corona from S4 nanoparticles. S2, S3 and P25 nanoparticles exhibited similar amounts of proteins in their corona. A slightly less important protein concentration was observed in the S1 corona.

For each nanoparticle type, a similar concentration of proteins was found in the coronas formed either in cDMEM or cRPMI (no statistically significant differences).

3.2. Profile of proteins adsorbed at the surface of the nanoparticles by gel electrophoresis

Fig. 4 illustrates the protein profile of the corona of the different nanoparticle types. The picture is representative of the three experiments performed.

Both in cDMEM and cRPMI we clearly observed that the corona of S2, S3 and P25 had very similar protein profiles, S1 presented a slightly lower amount of proteins whereas S4 corona exhibited the smallest protein content. These results are in perfect agreement with those of protein quantification (Fig. 3). In qualitative terms, interestingly and as highlighted by the rectangles on Fig. 4, we could observe that some proteins largely bound to the nanoparticles were not necessarily the most abundant in the culture medium (control lane).

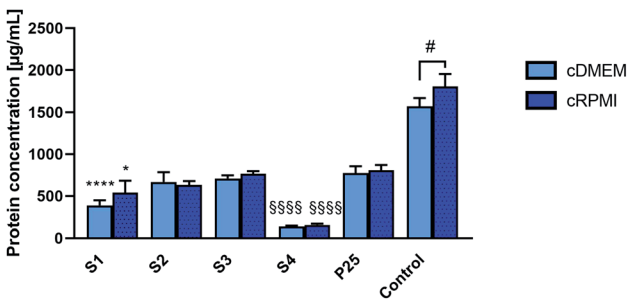

Fig. 3 Concentrations of proteins eluted from the protein corona of S1, S2, S3, S4 and P25 nanoparticles that were incubated either in cDMEM or cRPMI. Controls are cDMEM or cRPMI alone. Results are means of 3 independent experiments (except for S3 where we did not have enough nanoparticle sample to perform the last repetition so results are means of 2 independent experiments for this sample), standard deviation is also indicated. Statistically different from P25 (*) $P < 0.05$, (****) $P < 0.0001$. Statistical difference between S2 and S4 (§§§§) $P < 0.0001$. Statistical difference between cDMEM and cRPMI (#) $P < 0.05$.

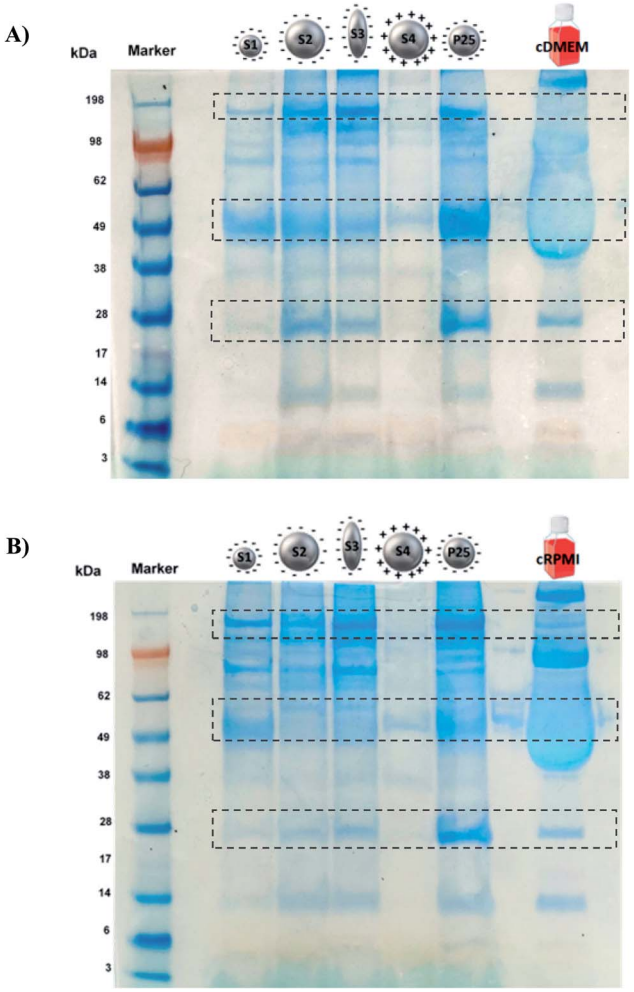

Fig. 4 SDS-PAGE of S1, S2, S3, S4 and P25 nanoparticles incubated either in cDMEM (A) or in cRPMI (B). As controls, the complete biological media alone were also run (last lane).

Table 4 Toxicity profiles observed for the studied TiO_2 nanoparticles incubated for 24 h in a lung coculture system (A549 epithelial cells/macrophages differentiated from THP-1 cells). Cytotoxicity was evaluated by assessing cell viability with Trypan blue assay. Pro-inflammatory response was assessed by the production level of the IL-8 and TNF-α pro-inflammatory cytokines. Oxidative stress was determined by the assessment of the ROS produced

	Cytotoxicity	Pro-inflammatory response	Oxidative stress
S1	+	+	–
S2	++	+	–
S3	++++	++	–
S4	++	++	–
P25	+++	++	–

3.3. Nanoparticles toxicity profiles

Table 4 reports the cytotoxicity patterns of the different nanoparticle types as previously assessed.[9]

We clearly observed different patterns of toxicity depending on the nanoparticle considered in relation with its physicochemical characteristics.[9]

4. Discussion

Fig. 5 summarizes the findings of this paper as well as previous data for discussion.

4.1. Impact of the nanoparticle physicochemical features on the formation of the protein corona

It has been extensively reported in the literature that the nanoparticle physicochemical features play a key role in the formation of the protein corona, especially, size, shape, surface charge and hydrophobicity.[10–21,43] In this study, by comparing the protein corona formation around 5 types of TiO_2 nanoparticles differing in size, shape, surface charge and agglomeration state, we aimed to shed light on the respective influence of such parameters.

By comparing S1 and P25 we could highlight the influence of nanoparticle size/SSA on the formation of the protein corona. We observed that smaller S1 nanoparticles (15 nm) showed a slightly less important amount of proteins in their corona compared to bigger P25 nanoparticles. This observation can be easily explained by the fact that when nanoparticle size varies, the curvature of the nanoparticle–protein interface is altered consequently affecting the protein adsorption at the nanoparticle surface. Similarly, a change in nanoparticle size/SSA induces an alteration of the deflection angle between adjacent proteins, thus when the size of the nanoparticle decreases, more steric repulsion occurs between the proteins of the corona.[12] In other words, smaller nanoparticles increase the deflection angle of the proteins and have a higher curvature than bigger nanoparticles, which can strongly impact qualitatively and quantitatively the composition of the protein corona.[20] It has even been shown that highly curved surfaces (very small nanoparticles) can suppress protein adsorption to the point where it no longer occurs.[44] Moreover, Tenzer *et al.*[18] demonstrated that even a 10 nm particle size difference significantly determined the protein corona of silica nanoparticles.

The influence of the nanoparticle shape on the formation of the protein corona was investigated by comparing rod-shaped S3 and spherical P25 nanoparticles. The amount and profile of proteins in the corona were similar, suggesting no impact of the shape. This finding is not in agreement with previous studies where nanorods were reported to adsorb more proteins than nanospheres of similar size, thanks to their small curvature.[19,45] This discrepancy can be due to the fact that the nanoparticles used in these studies were of different chemical nature (gold and silica) and of different sizes (10 and 270 nm for nanospheres and 10–35 and 270–1100 nm for nanorods). The nanoparticle–surface area ratios used were also different (0.003 and 0.05 m^2 mL^{-1}). This argues for a complex picture where several parameters are concomitantly involved.

S2 and P25 nanoparticles exhibited similar pattern suggesting that nanoparticle agglomeration state does not play a major role in the formation of the protein corona.

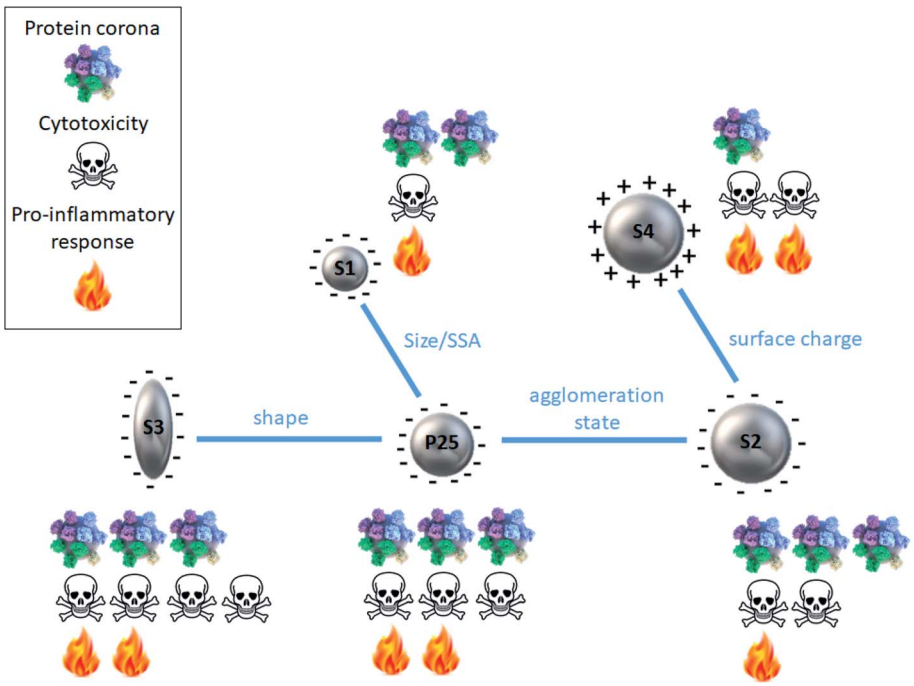

Fig. 5 Schematic summary of the protein corona and cytotoxicity profiles for each type of TiO_2 nanoparticle in relation with its physicochemical features.

On the contrary, by comparing the protein coronas of S2 and S4 (amine-functionalized form of S2) nanoparticles, we clearly observed a significant impact of the nanoparticle surface charge on the formation of a protein corona, confirming previous studies. However, it was quite surprising to observe that protein coronas were preferentially formed on negatively charged nanoparticles. Indeed, it is generally admitted that charged particles tend to adsorb more proteins than neutral nanoparticles.[12,16,17,20] The logical explanation is that, negatively charged particles attract positively charged proteins and *vice versa*. But, proteins contained in FBS are largely negative for a pH around 8, it should thus be reasonable to expect a larger protein binding to nanoparticles which surface is positively charged. However, this simplified statement does not fit all circumstances.[12,46,47] And our finding is consistent with those of Bewersdorff *et al.*[48] who reported that serum proteins preferably bound to negatively charged nanoparticles compared to positively charged ones. Tenzer *et al.*[18] also demonstrated that, at physiological pH (7.3), proteins in general with negative charge were preferentially bound by negatively charged SiO_2 nanoparticles irrespective of their relative plasma abundance. As nanoparticle surface chemistry has been shown to deeply influence the evolution and composition of a protein corona, it could be assumed that the nature of the chemical groups used for functionalization can contribute to controversial results. In our case, we can hypothesize a smaller protein corona for positively charged S4 nanoparticle as a result of a potential steric repulsion between the serum proteins and the amine groups of the APTES.

4.2. Impact of biological media on the formation of nanoparticle corona

As it is widely acknowledged that the protein corona formation also depends upon the biological environment[13,49–51] we compared the protein profiles obtained when TiO_2 nanoparticles were incubated in two types of standard cell culture media, DMEM and RPMI, supplemented by 10% FBS. From the protein quantification as well as the protein profiles observed on electrophoresis gels, we could conclude that the nature of the medium did not really impact the protein concentration of the corona of any nanoparticles. This finding is not in agreement with Maiorano *et al.*[36] who exposed various sized citrate-capped gold nanoparticles to cDMEM and cRPMI and reported that the protein corona formed in cDMEM was more abundant and stable compared to that formed in cRPMI. This discrepancy can be partly explained by the fact that systems are highly sensitive to even minor changes of some parameters. Here the chemical nature of the nanoparticle was different (TiO_2 and gold) and this calls for caution in generalizing conclusions.

We should also be careful in our conclusions as the zeta potential of nanoparticles varied greatly depending on the biological medium nanoparticles were incubated in (Table 2). Values were all negative when nanoparticles were in cDMEM and cRPMI, it even turned from positive (in water) to negative for S4. More important changes in zeta potential values were observed when nanoparticles were incubated in cDMEM compared to cRPMI. This could be due to a different protein composition of the two cell culture media resulting in the binding of proteins of various nature, differently charged on nanoparticles, making the zeta potential vary accordingly. Thus this observation is not inconsistent with a similar amount of proteins bound to nanoparticles irrespective of the biological medium (Fig. 3). Further investigations are needed, especially a qualitative characterization of the protein corona composition.

4.3. Correlation with the toxicity profile of nanoparticles

Among the numerous parameters that influence nanoparticle–cell interactions, the presence of a protein corona plays a key role. In this regard, Lesniak *et al.* showed that for identical particles and cells, under identical conditions, the nanoparticle–cell interactions and the biological outcomes could vary greatly in the presence or in the absence of a preformed corona in serum.[34] Because the protein corona defines the biological identity of nanoparticles and affects their biological response, it is now accepted that the types of proteins and their abundance on the nanoparticle surface encode information that predicts nanoparticle bioactivity.[24] And it can predict it more accurately than using models based only on the physicochemical properties of the nanoparticles.[20] Usually, the protein corona has a protective role against cell uptake and nanoparticles exhibiting a protein corona are less taken up than their bare counterparts.[30–33,35,37] The protein corona could decrease nanoparticle adhesion to the cell membrane due to the decreased surface-free energy after binding with proteins, thus decreasing particle–cell interactions and resulting in reduced uptake.[31,33] But some studies have shown the contrary, *i.e.* the presence of the protein corona enhancing nanoparticle uptake by cells.[52,53] These discrepancies can be explained by different cell internalization pathways: in the presence of a corona, non-specific uptake seems to be decreased whereas specific uptake seems to be promoted.[29,33,52,54] Because of a lower cell uptake the presence of a protein corona generally reduces the cytotoxic effects of nanoparticles.[14,25,27,29,32,34,36] Furthermore, the presence of a protein corona by masking the nanoparticle surface can mitigate its reactivity in interfacing cellular membranes and consequently prevent potential adverse effects.[34,55] At this point it is interesting to note that the five types of nanoparticles possessed comparable values in zeta potential in the culture media (Table 2), thus, the role of surface charge is expected to be screened by the protein corona. This observation seems to be in contradiction with the general knowledge that cationic nanoparticles tend to be more toxic than anionic nanoparticles. To reconcile these apparently diverging statements we should be very careful in the terms we use. Indeed, we should systematically specify if we are talking of the nanoparticle charge in cell culture medium (*i.e.* in the medium where the cytotoxicity assays are carried out and thus in the presence of the protein corona) or if we are talking of the pristine nanoparticle charge (as characterized after synthesis in DI water and thus in the absence of a protein corona). This crucial distinction is not

always made and can lead to misinterpretations. Finally, the presence of a protein corona can increase the safety of nanoparticles by inhibiting the generation of radical oxygen species by which several compounds exert their cytotoxic activity.[56]

In this context, the characterization of a nanoparticle protein corona is of paramount importance to better understand the mechanisms underlying its toxicity. As shown by Fig. 5, we were not able to evidence a clear relationship between protein corona pattern and the toxicity elicited by the nanoparticles. For instance, S4 exhibited the smallest protein corona and a significant cytotoxic activity. While S2, S3 and P25 had similar protein corona profiles, the intensity of the adverse effects they induced ranged from low to very high.

However, we should be cautious with this result as the nanoparticle doses used for the protein corona characterization and the cytotoxicity assays were different. Indeed, to allow comparison between the protein coronas of different nanoparticles, we used a constant total particle–surface area to biological medium volume ratio. We first tried concentrations equivalent to those used for cytotoxicity assays but we did not get enough proteins for analysis, therefore we increased the doses to get exploitable results. Such concentrations allowed us to conclude on the impact of the nanoparticle physicochemical features on the formation of the protein corona as discussed before. Although lower nanoparticle doses were used for cytotoxicity assays, we were able to rank the nanoparticles with respect to their toxicity and in Fig. 5 we reasoned in terms of relative and not absolute values making the comparison still meaningful. Similarly, another parameter to consider is the incubation time of the nanoparticles in the cell culture media (1 h in the present study of the protein corona and 24 h in the cytotoxicity assessment). This difference may result in a slightly different protein corona composition as this latter is known to evolve over time. Indeed, the proteins the most abundant in the medium and with high mobility first adsorb on the nanoparticle surface but they are progressively replaced by proteins exhibiting a higher affinity.[12,57] However, it seems to be a really fast process as Tenzer *et al.* demonstrated that an interaction between nanoparticle surface and plasma proteins is established as early as after 30 s of contact and that protein corona nature did not change over time.[17] It is thus reasonable to assume that protein corona composition remains quite stable after 1 h of nanoparticle/culture medium contact and we can confidently assume that it is representative of protein corona that would be observed after 24 h.

Furthermore, several assumptions can be made to explain the absence of clear correlation between the nanoparticle protein corona and toxicity. It is mainly related to our incomplete characterization of the protein corona. Indeed, because of technical challenges, we could only study the hard corona, composed of tightly bound proteins. The soft corona, consisting of less tightly bound proteins cannot be preserved during the analysis process. However, the soft corona represents the most external layer of proteins, which is thus likely to be in contact with biological systems. The unexplored role of soft protein corona may be a determinant factor for a better understanding of nanoparticle–cell interactions. One limitation of the present study was to consider the protein corona mainly through a quantitative aspect. In addition, we have to keep in mind that it is a preliminary study aiming to draw general patterns, to gain a first impression about the amount and composition of the corona proteins and that further investigations, including more sensitive techniques such as mass spectrometry analyses are required to refine our conclusions. Indeed, many studies evaluating the protein corona of nanoparticles by 1D or 2D gel electrophoresis are followed by mass spectrometry.[58,59] In particular, liquid chromatography-mass spectrometry (LC-MS) could be employed to determine protein corona composition qualitatively and quantitatively.

Indeed, to draw firm conclusion further investigations on the nature of the proteins should be conducted. It cannot be excluded that some proteins present at a minor level could be responsible for major biological consequences and *vice versa*.[29] Finally, it should be kept in mind that protein corona formation is very sensitive to many parameters both from the nanoparticle and the biological environment and minor changes in experimental conditions can have a deep impact on the protein corona formation/composition.[21,30] It is an interplay of different forces in a competing environment.[12]

5. Conclusions

Protein corona is a major issue for the study of the nanoparticle fate and consequences especially *in vivo* but *in vitro* studies are very useful to better understand what happens at a cellular level. In our model and experimental conditions the parameters influencing the protein corona formation are mainly nanoparticle size and surface charge, no clear impact of the shape and agglomeration state was observed. Although protein corona nature may undoubtedly influence nanoparticle cytotoxicity, no clear relationship was evidenced between the protein corona of 5 types of TiO_2 nanoparticles and the adverse effects they elicited in human lung cells. More comprehensive studies (considering qualitative/quantitative aspects, hard/soft corona) are needed to better understand the relationship between nanoparticle protein corona and toxicity.

Conflicts of interest

There are no conflicts to declare.

Funding

This research did not receive any specific grant from funding agencies in the public, commercial, or not-for-profit sectors.

References

1 E. Baranowska-Wójcik, D. Szwajgier, P. Oleszczuk and A. Winiarska-Mieczan, *Biol. Trace Elem. Res.*, 2020, **193**, 118–129.

2 IARC Working Group on the Evaluation of Carcinogenic Risks to Humans, International Agency for Research on Cancer and World Health Organization, *Carbon black,*

titanium dioxide, and talc, International Agency for Research on Cancer, Distributed by WHO Press, Lyon, France, Geneva, 2010.
3 M. Skocaj, M. Filipic, J. Petkovic and S. Novak, *Radiol. Oncol.*, 2011, **45**, 227–247.
4 M. S. Waghmode, A. B. Gunjal, J. A. Mulla, N. N. Patil and N. N. Nawani, *SN Appl. Sci.*, 2019, **1**, 310.
5 A. Weir, P. Westerhoff, L. Fabricius and N. von Goetz, *Environ. Sci. Technol.*, 2012, **46**, 2242–2250.
6 X. Chen and A. Selloni, *Chem. Rev.*, 2014, **114**, 9281–9282.
7 A. Albanese, P. S. Tang and W. C. W. Chan, *Annu. Rev. Biomed. Eng.*, 2012, **14**, 1–16.
8 A. Kurtz-Chalot, J. P. Klein, J. Pourchez, D. Boudard, V. Bin, G. B. Alcantara, M. Martini, M. Cottier and V. Forest, *J. Nanopart. Res.*, 2014, **16**, 1–15.
9 O. Kose, M. Tomatis, L. Leclerc, N.-B. Belblidia, J.-F. Hochepied, F. Turci, J. Pourchez and V. Forest, *Chem. Res. Toxicol.*, 2020, **33**, 2324–2337.
10 E. Casals and V. F. Puntes, *Nanomed*, 2012, **7**, 1917–1930.
11 T. Cedervall, I. Lynch, S. Lindman, T. Berggård, E. Thulin, H. Nilsson, K. A. Dawson and S. Linse, *Proc. Natl. Acad. Sci. U. S. A.*, 2007, **104**, 2050–2055.
12 D. Chen, S. Ganesh, W. Wang and M. Amiji, *Nanomed*, 2017, **12**, 2113–2135.
13 V. Forest, in *Nanoparticle–Protein Corona*, 2019, pp. 31–60.
14 M. P. Monopoli, D. Walczyk, A. Campbell, G. Elia, I. Lynch, F. B. Bombelli and K. A. Dawson, *J. Am. Chem. Soc.*, 2011, **133**, 2525–2534.
15 A. E. Nel, L. Mädler, D. Velegol, T. Xia, E. M. V. Hoek, P. Somasundaran, F. Klaessig, V. Castranova and M. Thompson, *Nat. Mater.*, 2009, **8**, 543–557.
16 D. E. Owens and N. A. Peppas, *Int. J. Pharm.*, 2006, **307**, 93–102.
17 S. Tenzer, D. Docter, J. Kuharev, A. Musyanovych, V. Fetz, R. Hecht, F. Schlenk, D. Fischer, K. Kiouptsi, C. Reinhardt, K. Landfester, H. Schild, M. Maskos, S. K. Knauer and R. H. Stauber, *Nat. Nanotechnol.*, 2013, **8**, 772–781.
18 S. Tenzer, D. Docter, S. Rosfa, A. Wlodarski, J. Kuharev, A. Rekik, S. K. Knauer, C. Bantz, T. Nawroth, C. Bier, J. Sirirattanapan, W. Mann, L. Treuel, R. Zellner, M. Maskos, H. Schild and R. H. Stauber, *ACS Nano*, 2011, **5**, 7155–7167.
19 R. M. Visalakshan, L. E. G. García, M. R. Benzigar, A. Ghazaryan, J. Simon, A. Mierczynska-Vasilev, T. D. Michl, A. Vinu, V. Mailänder, S. Morsbach, K. Landfester and K. Vasilev, *Small*, 2020, 2000285.
20 C. D. Walkey, J. B. Olsen, F. Song, R. Liu, H. Guo, D. W. H. Olsen, Y. Cohen, A. Emili and W. C. W. Chan, *ACS Nano*, 2014, **8**, 2439–2455.
21 C. D. Walkey and W. C. W. Chan, *Chem. Soc. Rev.*, 2012, **41**, 2780–2799.
22 G. Caracciolo, O. C. Farokhzad and M. Mahmoudi, *Trends Biotechnol.*, 2017, **35**, 257–264.
23 G. Caracciolo, S. Palchetti, V. Colapicchioni, L. Digiacomo, D. Pozzi, A. L. Capriotti, G. La Barbera and A. Laganà, *Langmuir*, 2015, **31**, 10764–10773.
24 M. P. Monopoli, C. Aberg, A. Salvati and K. A. Dawson, *Nat. Nanotechnol.*, 2012, **7**, 779–786.
25 C. Ge, J. Du, L. Zhao, L. Wang, Y. Liu, D. Li, Y. Yang, R. Zhou, Y. Zhao, Z. Chai and C. Chen, *Proc. Natl. Acad. Sci. U. S. A.*, 2011, **108**, 16968–16973.
26 P. Jain, R. S. Pawar, R. S. Pandey, J. Madan, S. Pawar, P. K. Lakshmi and M. S. Sudheesh, *Biotechnol. Adv.*, 2017, **35**, 889–904.
27 N. P. Mortensen, G. B. Hurst, W. Wang, C. M. Foster, P. D. Nallathamby and S. T. Retterer, *Nanoscale*, 2013, **5**, 6372–6380.
28 M. Pearson, V. V. Juettner and S. Hong, *Front. Chem.*, 2014, **2**, 108.
29 E. Brun and C. Sicard-Roselli, *Cancer Nanotechnol.*, 2014, **5**, 7.
30 P. Chandran, J. E. Riviere and N. A. Monteiro-Riviere, *Nanotoxicology*, 2017, **11**, 507–519.
31 X. Cheng, X. Tian, A. Wu, J. Li, J. Tian, Y. Chong, Z. Chai, Y. Zhao, C. Chen and C. Ge, *ACS Appl. Mater. Interfaces*, 2015, **7**, 20568–20575.
32 D. Docter, C. Bantz, D. Westmeier, H. J. Galla, Q. Wang, J. C. Kirkpatrick, P. Nielsen, M. Maskos and R. H. Stauber, *Beilstein J. Nanotechnol.*, 2014, **5**, 1380–1392.
33 A. Lesniak, A. Salvati, M. J. Santos-Martinez, M. W. Radomski, K. A. Dawson and C. Åberg, *J. Am. Chem. Soc.*, 2013, **135**, 1438–1444.
34 A. Lesniak, F. Fenaroli, M. P. Monopoli, C. Åberg, K. A. Dawson and A. Salvati, *ACS Nano*, 2012, **6**, 5845–5857.
35 A. Lesniak, A. Campbell, M. P. Monopoli, I. Lynch, A. Salvati and K. A. Dawson, *Biomaterials*, 2010, **31**, 9511–9518.
36 G. Maiorano, S. Sabella, B. Sorce, V. Brunetti, M. A. Malvindi, R. Cingolani and P. P. Pompa, *ACS Nano*, 2010, **4**, 7481–7491.
37 S. R. Saptarshi, A. Duschl and A. L. Lopata, *J. Nanobiotechnol.*, 2013, **11**, 26.
38 Z. J. Deng, M. Liang, M. Monteiro, I. Toth and R. F. Minchin, *Nat. Nanotechnol.*, 2011, **6**, 39–44.
39 D. Docter, U. Distler, W. Storck, J. Kuharev, D. Wünsch, A. Hahlbrock, S. K. Knauer, S. Tenzer and R. H. Stauber, *Nat. Protoc.*, 2014, **9**, 2030–2044.
40 D. Chen, J. Shi, J. Yan, Y. Wang, F. Yan, S. Shang and J. Xue, *Chem. Res. Chin. Univ.*, 2008, **24**, 362–366.
41 J. Zhao, M. Milanova, M. M. C. G. Warmoeskerken and V. Dutschk, *Colloids Surf., A*, 2012, **413**, 273–279.
42 S. Brunauer, P. H. Emmett and E. Teller, *J. Am. Chem. Soc.*, 1938, **60**, 309–319.
43 J. Piella, N. G. Bastús and V. Puntes, *Bioconjugate Chem.*, 2017, **28**, 88–97.
44 I. Lynch and K. A. Dawson, *Nano Today*, 2008, **3**, 40–47.
45 J. E. Gagner, M. D. Lopez, J. S. Dordick and R. W. Siegel, *Biomaterials*, 2011, **32**, 7241–7252.
46 V. Forest, M. Cottier and J. Pourchez, *Nano Today*, 2015, **10**, 677–680.
47 V. Forest and J. Pourchez, *Mater. Sci. Eng., C*, 2017, **70**, 889–896.
48 T. Bewersdorff, J. Vonnemann, A. Kanik, R. Haag and A. Haase, *Int. J. Nanomed.*, 2017, **12**, 2001–2019.

49 C. Gräfe, A. Weidner, M. V. D. Lühe, C. Bergemann, F. H. Schacher, J. H. Clement and S. Dutz, *Int. J. Biochem. Cell Biol.*, 2016, **75**, 196–202.
50 V. Mirshafiee, R. Kim, M. Mahmoudi and M. L. Kraft, *Int. J. Biochem. Cell Biol.*, 2016, **75**, 188–195.
51 D. Pozzi, G. Caracciolo, A. L. Capriotti, C. Cavaliere, G. La Barbera, T. J. Anchordoquy and A. Laganà, *J. Proteomics*, 2015, **119**, 209–217.
52 Y. Qiu, Y. Liu, L. Wang, L. Xu, R. Bai, Y. Ji, X. Wu, Y. Zhao, Y. Li and C. Chen, *Biomaterials*, 2010, **31**, 7606–7619.
53 M. M. Yallapu, N. Chauhan, S. F. Othman, V. Khalilzad-Sharghi, M. C. Ebeling, S. Khan, M. Jaggi and S. C. Chauhan, *Biomaterials*, 2015, **46**, 1–12.
54 F. Zhao, Y. Zhao, Y. Liu, X. Chang, C. Chen and Y. Zhao, *Small*, 2011, **7**, 1322–1337.
55 C. Corbo, R. Molinaro, A. Parodi, N. E. Toledano Furman, F. Salvatore and E. Tasciotti, *Nanomed*, 2016, **11**, 81–100.
56 H. Yin, R. Chen, P. S. Casey, P. C. Ke, T. P. Davis and C. Chen, *RSC Adv.*, 2015, **5**, 73963–73973.
57 L. Vroman and A. L. Adams, *Surf. Sci.*, 1969, **16**, 438–446.
58 M. Wang, O. J. R. Gustafsson, E. H. Pilkington, A. Kakinen, I. Javed, A. Faridi, T. P. Davis and P. C. Ke, *J. Mater. Chem. B*, 2018, **6**, 6026–6041.
59 F. S. M. Tekie, M. Hajiramezanali, P. Geramifar, M. Raoufi, R. Dinarvand, M. Soleimani and F. Atyabi, *Sci. Rep.*, 2020, **10**, 9664.